Issue 1: Hydrogen as cause of the flaws

When discussing hydrogen flaking as the most likely cause of the indications detected in the Doel 3 and Tihange 2 reactor pressure vessels, the Safety Cases of Doel 3 and Tihange 2 (version dated 5 December 2012) mention that "*The measured hydrogen level in the liquid metal of around 1.5 ppm, could be above the threshold for hydrogen flaking, since the sulphur level is relatively low. AREVA recommends a conservative maximum allowed hydrogen content of 0.8 ppm.*"

From this information, the authors of [1] deduce that an amount of 61 ml/dm³ of H_2 is set free during the cooling of the material. After some calculations, and by assuming that there is no significant diffusion of hydrogen coming from the rest of the base metal towards the high flaw density areas, the authors of [1] conclude that hydrogen flaking cannot be the only cause of the flaws, and that another cause has resulted in flaking or that the flaws have been growing during time.

The reasoning used to conclude this is misleading, mainly because the two following assumptions are not correct:

- *an amount of 61 ml of H_2 is set free*: to our understanding, the authors of [1] make a confusion between the concept of hydrogen solubility in steel and the concept of the hydrogen content threshold to avoid hydrogen flaking;
- *there is no significant diffusion of hydrogen coming from the rest of the base metal towards the high flaw density areas*: hydrogen diffusion is on the contrary at the heart of the flaking formation.

More information is given below, especially to understand how hydrogen flakes develop.

As developed below, hydrogen flakes appear during the fabrication of heavy forgings, when these have a mean hydrogen content which exceeds some acceptable critical value or threshold. Different values can be found in the literature (mainly because it is dependent of the content of other chemical species, such as Sulphur), but typically, for modern clean steels, this threshold is considered to be about 0.8 ppm. This means that when the mean hydrogen content of the forging is below this threshold, hydrogen flakes will most probably not develop. On the other hand, when the hydrogen content is above this threshold, there is a high risk of hydrogen flaking in the forging. When such flakes develop, they generally appear in large quantities, even when the hydrogen content is only about 1.5 ppm. This is because the amount of hydrogen that will participate in this phenomenon is not equal to the difference between the mean hydrogen content of the ingot and the threshold of 0.8 ppm, as supposed by the authors of [1], and the reason is explained below.

The amount of hydrogen that can be contained in the steel is characterized by its solubility (which is a different concept from the threshold of 0.8 ppm). This solubility expresses the maximum amount of (atomic) hydrogen which can be dissolved into the material.

As illustrated by Figure 1, the solubility of (atomic) hydrogen is much higher in liquid steel than in the solid metal. Furthermore, the solubility in the solid steel depends on the phase: the hydrogen solubility in the γ-phase is higher than in the α-phase. At room temperatures, the hydrogen solubility is much smaller than 0.8 ppm.

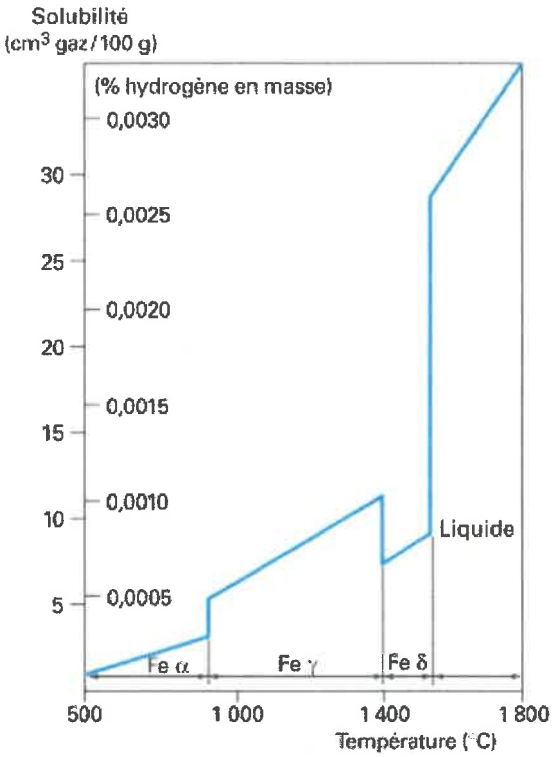

Figure 1. Temperature dependence of hydrogen solubility in iron

The solidification of the large castings is a complex metallurgical process and the resulting ingot is characterized by several particular regions, differentiated by their chemical composition. When liquid steel locally solidifies, for solubility reasons, alloying elements (solute) are rejected in the surrounding liquid, which become enriched in those elements. Thus, the first region to solidify in an ingot is poor in solute (negative segregation) and the last region to solidify is rich in solute (positive segregation). Local areas of highly solute-rich liquid can also form small channels rising to the top of the ingot and are termed A-segregates of ghost lines after their solidification. During solidification of the casting, hydrogen segregates to the surrounding liquid areas due to the difference in hydrogen solubility between the liquid steel and the solid steel. However, after the solidification, when the ingot is maintained at the high temperature at which the forging will be performed, the steel structure is austenitic (γ-phase). After forging, the forged component is cooled down but the resulting transformation from the γ-phase to the α-phase is not uniform in the whole volume of the component. Due to their higher enrichment in alloying elements, the segregated areas have a lower transformation temperature, which means that there is a time-lag between the transformation to ferrite of the unsegregated areas and that of the segregated areas. Unsegregated regions are first transformed to ferrite and due to the lower hydrogen solubility in α-phase, the hydrogen in the (ferritic) unsegregated regions diffuses to the (austenitic) segregated regions where it accumulates. When the segregated regions finally transform to ferrite, they become supersaturated in hydrogen, which precipitates in molecular form at trapping sites such as inclusions, grain boundaries and microvoids, building up an internal pressure. The ghost lines that are the most enriched areas are the last to transform to α-phase. So, the precipitation of molecular hydrogen occurs preferentially at the trapping sites in the ghost lines and in particular at the MnS inclusions.

It is generally accepted that the internal H_2 pressure at the trapping sites is not sufficient to cause micro-cracks (flakes). Additional stresses such as transformation stresses, local stress

concentrations around defects (inclusions) and deformation stresses during forging are believed to promote flaking. Moreover, another parameter promoting the occurrence of flaking is a cracking-sensitive microstructure. With regard to that, the ghost lines have a high content in alloying elements (e.g., C, Mn, P, Mo) that are quenching elements and are therefore more sensitive to quenching, which promotes the formation of a martensitic structure which, under untempered condition, has a brittle nature.
For all those reasons, when flaking is present in a forging, the flakes are located preferentially in the ghost lines.

Calculations to estimate the final dimension of the flakes and the hydrogen pressure needed to form these cracks are very difficult, since they should take into account dynamical effects due to the cracking itself as well as deformation stresses due to the forging process (as it is known that these latter play an important role in the hydrogen flaking mechanism). The results obtained by the simulations made in [1] and which did not take into account these effects are thus questionable.

Finally, we can convince ourselves that hydrogen flakes can form in large quantities, even if the measured hydrogen level seems quite small. Indeed, the VB395, which has not been used in service, had a relatively similar measured hydrogen level and destructive testing showed that it contained large quantities of hydrogen flakes having similar dimensions as the ones lying in the Doel 3 and Tihange 2 reactor pressure vessels (RPV).

Issue 2: The absence of a consolidated theory for material with a high density of cracks

It is known that the driving force acting on a given crack (stress intensity factor) can be significantly affected by the presence of one or more cracks in the close neighbourhood. Depending on the relative position and orientation of the neighbouring cracks, this interaction effect can either increase or decrease the stress intensity factor. When assessing the fracture strength of structures affected by multiple cracks, the classical procedure used by the fitness-for-service Codes for avoiding the calculation of the interaction effect between neighbouring cracks is to replace the closely-spaced interacting flaws by one single larger flaw that envelopes those flaws. Such a procedure is acceptable subject to the condition that the fracture potential of each interacting flaw is conservatively assessed by the fracture potential of the larger enveloping flaw. Otherwise stated, the stress intensity factor of the enveloping flaw shall be larger than the stress intensity factor of each individual flaw taking into account the interaction effect. The usual practice is to define interaction criteria or proximity rules that are used to determine which flaws are not to be assessed separately as isolated flaws but are to be merged.

The damage of the Doel 3 and Tihange 2 RPV core shells is characterized by a high number of closely-spaced flaw indications. Due to the presence of multiple closely-spaced flaws, the local stress field in the zone containing the flaws may be significantly affected. As the stress intensity factors are governed by the stresses in the vicinity of the cracks, the perturbation to the local stress field is the underlying cause of the interaction effect. An adequate and conservative assessment of the interaction effect between multiple flaws is therefore a key step in the evaluation of the fracture behaviour of the RPV core shells.

The definition of the proximity rules using 3D flaw calculations is based, as mentioned by [1], on the results of a research work performed by K. Hasegawa showing that two non-aligned

thru-wall cracks in a flat plate will connect to each other once the brittle fracture is initiated at the condition that the interaction factor is greater than 1.06. The interaction factor quantifies the increase of the stress intensity factor for a flaw due to the interaction with another flaw. While recognizing that those results have provided the technical basis for the definition of the revised grouping criteria of Section XI of the ASME B&PV Code, Bel V remained reluctant to the basic idea of requiring grouping of two flaws when coalescence of these two flaws is expected in the brittle fracture process. To Bel V understanding, the objective of calculating the stress intensity factor and comparing it to the fracture toughness is to prevent the crack initiation. An accurate estimate of the value of the stress intensity factor is therefore required. Due to the interaction effect, calculating the stress intensity factor of a crack as an isolated crack while being in the neighbourhood of other cracks may be non-conservative. For practical purpose however, it may be found necessary to define a threshold below which the interaction effect should not be considered in fracture assessment. The threshold of the interaction factor should not be too low to account for the accuracy in the evaluation of the stress intensity factor but also not too high. A threshold value of 1.06 for the interaction factor appeared acceptable to Bel V.

One of the main concerns raised by Bel V in his evaluation of the revised proximity rules was the assumption made by Electrabel that the interaction between two neighbouring flaws was not affected by the presence of other flaws in the close neighbourhood. By doing so, Electrabel assumed that the interaction between two neighbouring flaws in a cluster was not affected by the presence of the other flaws in the cluster. Otherwise stated, Electrabel assumed that the local stress field around two neighbouring flaws in a cluster was not affected by the other flaws in the cluster. A potential consequence of taking into account the impact of other flaws in the neighbourhood would be the enlargement of the interaction domain, the latter being defined as the limiting distances between two flaws for which interaction has to be considered. Bel V recognized that the boundaries of the interaction domain for two flaws had been enlarged by 20% to define the proximity rules but he wondered whether that arbitrary enlargement was sufficient to cover the potential enlargement of the interaction domain when other flaws in the close neighbourhood of the two analysed flaws were considered.

Electrabel and Bel V agreed that an acceptable answer to that concern was to show by using multi-flaw 3D analyses of typical flaw configurations from the Doel 3 RPV lower core shell that the enlargement by 20% was actually not necessary. In other words, in regions affected by closely-spaced flaws, some groups of flaws defined by using the proposed proximity rules are expected to contain more flaws than the groups that would be defined by using proximity rules without the 20% enlargement. For those groups, the enlargement could be considered as not necessary if the maximum equivalent stress intensity factor Keq in the group defined using the proposed proximity rules was not significantly higher than the maximum equivalent intensity factor Keq in the group defined without 20% enlargement. Otherwise stated, the consideration of additional neighbouring flaws did not increase significantly the maximum equivalent intensity factor Keq. Two groups of flaws belonging to the Doel 3 lower core shell were considered as typical flaws for illustrating the non-necessity of enlarging by 20% the interaction domain. When using the proposed proximity rules, the first group contained 3 flaws and the second group contained 9 flaws. When using proximity rules without enlargement of the interaction domain by 20%, the number of flaws in those groups was reduced to 2 and 5 flaws respectively. However, it was found that the value of the maximum equivalent intensity factor Keq was not significantly changed. Adding one flaw in the first group increased the maximum equivalent intensity factor Keq by 0.01% and in the second

group, adding 4 flaws increased the maximum equivalent intensity factor Keq by 0.34%. Bel V concluded that for the flaw configurations in the Doel 3 and Tihange 2 RPVs, the interaction between two neighbouring flaws was not significantly affected by the presence of other flaws in the close neighbourhood.

Bel V concluded that the use of the proximity rules for quasi-laminar flaws was acceptable but he also emphasized that the conclusion only applied to the flaw configurations detected in the Doel 3 and Tihange 2 RPV core shells.

It should be highlighted that if the grouping methodology which led to Code Case N-848 was indeed used in the Safety Case of 2012 and constituted an important part of the structural integrity demonstration, this was not the case for the Safety Case of 2015. In particular, the grouping methodology of Code Case N-848 is based on 2D Finite Elements calculations, whereas the grouping methodology of the 2015 Safety Case is based on 3D calculations. Moreover, the critical groups of flaws as well as a sample of appropriately selected other groups have been specifically studied in refined analyses in which the flaws were not grouped, which means that the grouping step has not the importance given by [1].

Note finally that the UT inspection of the RPV core shells with straight beam transducers does not allow to identify any hypothetical radial connection between flakes located at slightly different depths (called branched flaws in [1]). In order to reject that assumption, the data recorded by the eight 45° transducers installed on the UT inspection tool were analysed in order to detect any such connections. Bel V acknowledged that no radial connections between flakes were detected. Destructive examinations of the VB395 have confirmed the absence of such radial connections even in high flaw density regions.

Minor issues

1. **Temperature gradient over the vessel wall in the flaw zone.**

   For circumferential or axial planar flaws that are perpendicular to the RPV surface, it may be assumed without any significant loss of accuracy in the calculation that the temperature distribution is not affected by the presence of the flaws. For quasi-laminar flaws such as the flakes, their orientation with respect to the (radial) heat flux makes that the same conclusion might be invalid. Indeed, depending on their thermal resistance, the quasi-laminar flaws may act as thermal barriers. As a result, the temperature distribution in the wall thickness may depart from the normal one (i.e., without flaw) and the temperature gradient in the vicinity of the flaws may potentially be higher. This concern may be of importance for the 20mm thick zone beneath the cladding where the thermal stresses due to the small break loss of coolant accident (small LOCA) contribute significantly to the stress intensity factor.

   Postulating the thermal conductance of the flakes equal to the thermal conductance of the sound material is an idealization of the actual physical condition because the thermal contact resistance between the contacting surfaces of the flakes should at least be considered. In order to better substantiate the effect of the flakes on the thermal distribution, Bel V asked Electrabel in the frame of the Safety Case to investigate the consequences of the other bounding assumption, i.e., no heat transfer thru the flakes, on the flaw assessment.

As an answer to the Bel V request, Electrabel provided the results of the finite-element MORFEO-CRACK analysis of a 2D model of a RPV sector. The model includes two closely-spaced flaws located close to the cladding. In addition to the pressure, the boundary conditions of the model include the small-break LOCA temperature transient at the inner surface. The model considers no heat transfer through the flakes by modelling the flakes with a small opening in the mesh. In order to assess the impact of the assumption of no-heat transfer through the flakes, a second analysis is performed on the same model, but assuming perfect heat transfer through the flakes. The results given by Electrabel are those corresponding to the time in the transient for which the margin to the acceptance criterion is the lowest. When compared to the case of perfect heat transfer through the flakes, the maximum stress intensity factor at the front of the flaws (assumed to have a tilt angle of 8°) is increased by about 10%. As expected, that increase is due to the local increase of the thermal gradient at the crack front and between the flaws. However, the impact on the flaw assessment is lower. Indeed, as the flaws act as thermal barriers, the temperature at the crack front is slightly increased and, as a result thereof, the material fracture toughness is slightly increased also.

Recognizing (i) that the 2D model overestimates somewhat the perturbation to the temperature field and (ii) that, as a result at least of the radiation heat transfer, the actual heat transfer through the flakes has definitely a non-null value even if the flakes are open, Bel V concludes that the potential underestimation of the crack driving force due to the lower heat transfer through the flakes should have a low impact of the flaw assessment.

2. Boundary conditions for flaw simulation in shell segment

Due to the quasi-laminar nature of the flakes, it is not expected that they will have a significant impact on the hoop stresses. Also, it has been shown that for the load cases to be considered, even with this high flaw density, the stress field is significantly affected only in the very close neighbourhood of each flake. On a macroscopic scale flakes have no influence on the stress field, see also answer to issue 2.

3. Vibration levels are unknown

Vibration levels are insignificant.

4. Opinion of Westinghouse

AREVA, which has bought the Westinghouse license and which is also a nuclear power plant designer, has been strongly involved in the assessment.
Moreover, as an answer to the return of experience of Doel 3 and Tihange 2, Westinghouse participated in the elaboration of [2], which is a bounding safety assessment for a vessel postulated to have a large number of quasi-laminar indications in the beltline shell forgings. The bounding assessment included a Probabilistic Fracture Mechanic analysis of the U.S. PWR with highest mean reference temperature in a beltline ring forging at the end of a sixty-year license. This study determined that the incremental risk would be a factor of 10 below the risk criteria set by the USNRC. Therefore, the potential for vessel failure was considered acceptably low. This conclusion has been assessed and endorsed by the USNRC [3].

Minor correction
In §1: the primary water is circulated by pumps through the steam generators with a volume flow of 21.000 m^3/h, instead of 21 m^3/h.

References

[1] "Critical reflection about the integrity of the reactor vessels of the Doel 3 and Tihange 2 nuclear power plants", René Boonen and Jan Peirs, 8 December 2016

[2] "Materials Reliability Program: Evaluation of the reactor vessel beltline shell forgings of operating U.S. PWRs for quasi-laminar indications (MRP-367)", October 2013

[3] "Technical assessment of potential quasi-laminar indications in reactor pressure vessel forgings", USNRC, 8 September 2015, ADAMS ML15282A218